



Minimum Standardized Uptake Value from Quantitative Bone Single-Photon Emission Computed Tomography/Computed Tomography for Evaluation of Femoral Head Viability in Patients with Femoral Neck Fracture

Hyun Gee Ryoo¹ · Won Woo Lee^{1,2}  · Ji Young Kim³ · Eunjung Kong⁴ · Woo Hee Choi⁵ · Joon-kee Yoon⁶ · K-SPECT Group

Received: 8 April 2019 / Revised: 16 May 2019 / Accepted: 7 June 2019 / Published online: 22 June 2019

© Korean Society of Nuclear Medicine 2019

Abstract

Purpose Bone single-photon emission computed tomography/computed tomography (SPECT/CT) has been widely used for evaluation of femoral head viability in patients with femoral neck fracture. The current study aimed to investigate utility of standardized uptake value (SUV) from quantitative bone SPECT/CT for assessment of femoral head viability.

Methods From March 2015 to November 2018, quantitative bone SPECT/CT was performed in 9 patients with non-viable femoral head post femoral neck fracture and in 31 controls. Maximum (SUV_{max}), mean (SUV_{mean}), and minimum standardized uptake values (SUV_{min}) were measured over femoral head and neck. Mann-Whitney *U* test with Bonferroni correction was used to compare SUVs of ipsilateral and contralateral femurs from femoral neck fracture patients with those of control femurs.

Results As for femoral head viability, SUV_{max} and SUV_{mean} were not significantly decreased in non-viable femoral heads compared to those in controls. Only the SUV_{min} was significantly reduced in non-viable femoral heads (mean ± standard deviation, 0.57 ± 0.38) than in controls (0.95 ± 0.26, *p* = 0.006) and contralateral femoral heads (1.36 ± 0.59, *p* = 0.008). The cutoff SUV_{min} of 0.61 (g/mL) yielded a sensitivity of 77.8% and specificity of 87.1% for detection of non-viable femoral heads (*p* = 0.006). Contralateral femoral necks of the femoral neck fracture patients showed significantly higher SUV_{mean} and SUV_{min} (3.17 ± 1.20 and 1.64 ± 0.63) than those of controls (2.32 ± 0.53 and 1.04 ± 0.27; *p* = 0.021 and *p* = 0.002, respectively), which seemed to reflect weight bearing effect or metabolic derangement.

Conclusions The non-viable femoral heads from the femoral neck fracture showed significantly reduced SUV_{min}. Quantitative bone SPECT/CT holds promise for objective evaluation of femoral head viability.

Keywords Femur · Fracture · Single-photon emission computed tomography · Computed tomography · Quantitation · Standardized uptake value

Electronic supplementary material The online version of this article (<https://doi.org/10.1007/s13139-019-00600-2>) contains supplementary material, which is available to authorized users.

✉ Won Woo Lee
wwlee@snu.ac.kr

¹ Department of Nuclear Medicine, Seoul National University Bundang Hospital, Seoul National University College of Medicine, 82, Gumi-ro 173 Beon-gil, Bundang-gu, Seongnam-si, Gyeonggi-do 13620, South Korea

² Institute of Radiation Medicine, Medical Research Center, Seoul National University, Seoul, South Korea

³ Department of Nuclear Medicine, Hanyang University Guri Hospital, Hanyang University College of Medicine, Seoul, South Korea

⁴ Department of Nuclear Medicine, Yeungnam University Medical School and Hospital, Daegu, Gyeongsangbuk-do, South Korea

⁵ Division of Nuclear Medicine, Department of Radiology, St. Vincent's Hospital, College of Medicine, The Catholic University of Korea, Seoul, South Korea

⁶ Department of Nuclear Medicine & Molecular Imaging, Ajou University School of Medicine, Woldeukeom-ro, Suwon-si, South Korea

Introduction

Bone scintigraphy using technetium-99m methylene diphosphonate (Tc-99m MDP), Tc-99m dicarboxypropane diphosphonate (DPD), and Tc-99m hydroxymethylene diphosphonate (HDP) has been widely used for the evaluation of femoral head viability in patients with femoral neck fracture [1, 2]. Since the two-dimensional planar imaging in traditional bone scintigraphy had limitations in properly evaluating the femoral head, pin-hole collimator imaging or three-dimensional single-photon emission computed tomography (SPECT) evolved for accurate evaluation of femoral head viability [3, 4]. The integration of X-ray computed tomography (CT) with SPECT, generating the hybrid imaging mode of SPECT/CT, has further improved the utility of bone scintigraphy for femoral head assessment [5, 6]. Thus, bone SPECT/CT is now advocated as a useful assessment tool for patients with femoral neck fracture. However, femoral head viability has been determined using qualitative or semi-qualitative scores on the uptake degree (i.e., degree of photopenia) of the bone imaging agents [4–7].

Truly quantitative and unbiased parameters are now being introduced in the field of SPECT/CT [8, 9]. Due to the sophisticated image reconstruction algorithms of attenuation correction, scatter correction, and resolution recovery (correction of the distance variation between the patient and detector), state-of-the-art SPECT/CT scanners can readily provide a standardized uptake value (SUV) that is almost equivalent to the positron emission tomography (PET)-derived SUV [10–18]. As the assessment of femoral head viability is an important indication of bone SPECT/CT, we attempted to apply the quantitative SPECT/CT technique for patients with femoral neck fracture. Our primary goal was to demonstrate the usefulness of the SUV for objective determination of femoral head viability.

Materials and Methods

Patients

From March 2015 to November 2018, consecutive patients with unilateral femoral neck fracture and control patients, who underwent quantitative bone SPECT/CT at the Department of Nuclear Medicine of Seoul National University Bundang Hospital, were enrolled. The patients with femoral neck fracture were proven to have osteonecrosis of the corresponding femoral head during subsequent total hip replacement surgery. The bone SPECT/CT was performed median 4 days (range, 1–12 days) after the fracture events, while the interval between femoral neck fracture and surgery was median 6 days (range, 3–13 days). Conversely, the control patients underwent bone SPECT/CT because of low back pain, hip pain, multiple joint pain, or acute lower extremity

lymphedema aggravation without evidence of femoral head/neck pathology, which was proved by magnetic resonance imaging (MRI) ($n = 3$) 41, 48, and 1002 days after SPECT/CT or clinical follow-up ($n = 28$) until median 313 days (range, 14–1435 days) after SPECT/CT. This study was retrospectively designed and approved by the institutional review committee of the hospital. The need for informed consent was waived by the committee.

Quantitative Bone SPECT/CT

The protocol of quantitative bone SPECT/CT is available in the previously published literature [10, 12, 18]. First, we performed a phantom study for cross-calibration between a dose calibrator (CRC-15R; CAPintec) and SPECT/CT scanners (NMCT/670 and NMCT/670Pro; GE Healthcare): the system sensitivity (the converting factor for radio-activity from counts/min) for NMCT/670 was 152.5 until July 2017 and then updated to 151.8 since September 2017, while the equivalent for NMCT/670pro was 152.8 cpm per μCi throughout the study. Second, SPECT/CT images were acquired 2–3 h after injection of 20 mCi Tc-99m HDP. For calculation of the quantitative parameters, the following data were recorded in every study: radioactivity and measurement time before and after injection, imaging start time, and patients' body weight. Initially, the planar images over the hip area were acquired. Then, SPECT acquisition was performed under the following imaging conditions: low-energy high-resolution collimation, energy window peak at 140 KeV (20% windowing of 126–154 KeV), scatter window at 120 KeV (10% windowing of 115–125 KeV), step and shoot mode (10 s/step, 3° angle, 60 steps/detector), body contouring, and zoom factor of 1.14 or 1.5. Next, helical CT for image co-registration and attenuation correction was obtained using the following parameters: tube voltage 120 KVp, tube current 60–210 mA with auto mA function with noise level 20, X-ray collimation 20 mm ($= 16 \times 1.25$), helical thickness 2.5 mm, table speed 37 mm/s, table feed per rotation 18.75 mm/rot, tube rotation time 0.5 s, and pitch 0.938:1. SPECT images were reconstructed using vendor-provided software (Preparation for Q.Metrix; GE Healthcare) using an iterative ordered subset expectation maximization (OSEM) algorithm with 2 iterations and 10 subsets into a matrix of 128×128 with slice thickness of 2.95 mm or 3.88 mm. A post-reconstruction filter (Butterworth with frequency 0.48 and order 10) was applied. Triple corrections (CT-based attenuation correction, dual-energy window-based scatter correction, and resolution recovery) were applied during SPECT reconstruction. CT images had been reconstructed using an adaptive statistical iterative reconstruction algorithm (ASiR; GE Healthcare) with bone plus filtering function into an image matrix of 512×512 with a slice thickness of 2.5 mm.

Quantitative Parameters from the SPECT/CT

The quantitative parameters investigated in the study were the maximum SUV (SUV_{max}), mean SUV (SUV_{mean}), and minimum SUV (SUV_{min}).

$$\text{SUV}_{\max} = \frac{\text{Maximum radioactivity/Volume of voxel}}{\text{Injected radioactivity/Body weight}} \text{ (g/mL)}$$

$$\text{SUV}_{\text{mean}} = \frac{\text{Total radioactivity/Volume of region}}{\text{Injected radioactivity/Body weight}} \text{ (g/mL)}$$

$$\text{SUV}_{\min} = \frac{\text{Minimum radioactivity/Volume of voxel}}{\text{Injected radioactivity/Body weight}} \text{ (g/mL)}$$

The above parameters were calculated over the femoral head and neck using vendor-provided quantitative software (Q.Metrix; GE Healthcare). The voxel volume in the current study was $3.2\text{--}7.3 \times 10^{-3}$ mL.

Segmentation of Femoral Head and Neck

Volumes-of-interest (VOIs) for each femoral head and neck were determined using co-registered coronal CT images. For the femoral head VOI, the region-of-interest (ROI) was manually drawn slice-by-slice along the upper contour of the femoral head and lower line of the epiphyseal plate (Fig. 1a). Approximately 20–25 ROIs were required to cover the whole volume of the femoral head (Fig. 1c). For the femoral neck VOI, 5 rectangles bordering the head-neck junction and intertrochanteric line were first placed with a regular interval over the femoral neck (Fig. 1b). The rectangles were interpolated and the femoral neck VOI was then semi-automatically segmented using the bone density inside the interpolated rectangles (Fig. 1c).

Statistical Analysis

An expert statistician from the institutional medical research collaborating center helped analyze, interpret, and present the data. Values were expressed as mean \pm standard deviation (SD). For the control patients, the SUVs from bilateral femurs were first averaged because there was no significant difference of SUVs between two side of the femurs (Supplemental tables), and then compared with those from patients. The Fisher's exact test was performed to test the difference in sex proportion between patients with femoral neck fracture and control patients. The Mann-Whitney *U* test was performed for age comparisons between patients with femoral neck

fracture and control patients. Comparisons of femoral head parameters between femoral neck fracture patients and control patients were performed using the Mann-Whitney *U* test, and the obtained *P* values were multiplied by two according to the Bonferroni correction for the adjustment of type I errors from multiple comparisons (i.e., non-viable femoral head vs control group, contralateral femoral head vs control group). Wilcoxon's signed rank test was performed to compare parameters between non-viable femoral head and intact contralateral femoral head. Comparisons of femoral neck parameters between patients with femoral neck fracture and control patients were performed using the Mann-Whitney *U* test. ROC (receiver-operating characteristic) analysis was conducted to determine the optimal cutoff value for disease identification. Statistical tests were performed using SPSS version 25 (IBM, Armonk, NY, USA), and a *P* value lower than 0.05 was considered statistically significant.

Results

Patient Characteristics

Nine patients with unilateral femoral neck fracture (male/female = 3:6, age = mean \pm SD, 79.3 ± 7.6 years [range, 69–91 years]) and 31 control patients (male/female = 7:24, age = 45.7 ± 14.3 years [range, 22–76 years]) were included in the present study. Among the nine patients with femoral neck fracture, eight patients had recent history of trauma and one patient had unknown cause of fracture. The patients with femoral neck fracture were significantly older than the controls ($p < 0.001$), but the sex proportion was similar ($p > 0.05$). All nine patients with femoral neck fractures showed complete cold defect of total femoral heads above femoral neck fractures on visual assessment of SPECT/CT.

SPECT/CT Parameters of the Femoral Head

For the SUV_{max}, no significant difference was observed among control (mean \pm SD, 4.94 ± 0.97), non-viable (6.60 ± 3.74), and contralateral (6.21 ± 1.90) femoral heads ($p > 0.05$) (Fig. 2a). For the SUV_{mean}, the non-viable femoral heads did not have a significant difference (1.98 ± 0.68) from that in controls (2.61 ± 0.63 , $p = 0.056$), but showed a significant decrease compared to the contralateral femoral heads (3.44 ± 1.07 , $p = 0.008$). In fact, the contralateral femoral heads had a significantly higher SUV_{mean} than that in the controls ($p = 0.048$) (Fig. 2b). Interestingly, the non-viable femoral heads readily showed a decrease in SUV_{min} compared to that in the controls and contralateral femoral heads; SUV_{min} was significantly and consistently reduced in the non-viable femoral heads (0.57 ± 0.38) compared to that in the controls (0.95 ± 0.26 , $p = 0.006$) and contralateral femoral heads (1.36 ± 0.59 ,

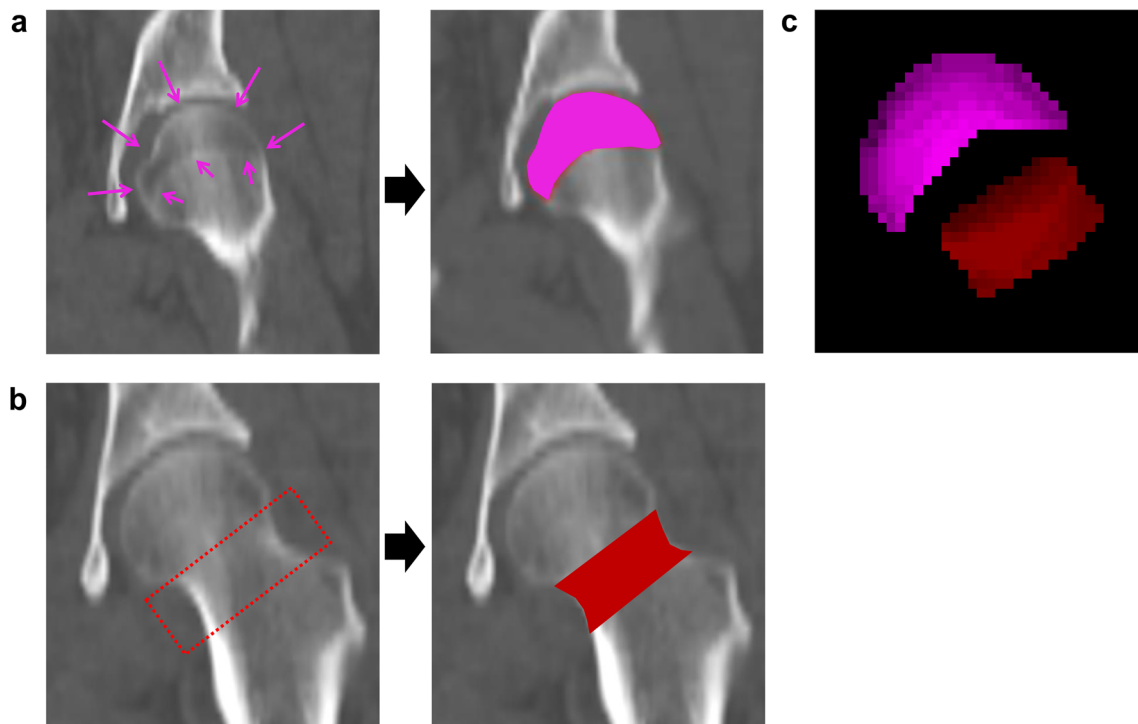


Fig. 1 Segmentation of the femoral head and neck. **a** ROIs were manually drawn over the femoral head. Upper contour (long arrows) and epiphyseal plate line (short arrows) were used as the anatomical reference. Approximately 20–25 ROIs were required to cover the femoral head. **b** Five rectangles bordering the head-neck junction and

intertrochanteric line were placed at regular intervals and then interpolated. The femoral neck was semi-automatically segmented by the bone density inside the interpolated rectangles. **c** VOIs for the femoral head and neck. ROIs, regions-of-interest; VOIs, volumes-of-interest

$p = 0.008$) (Fig. 2c; Table 1). The failure of the non-viable femoral heads to show considerably reduced SUVmax and SUVmean even with an apparently lower uptake by visual assessment was attributed to spill-over effects from surrounding bony structure. Since the femoral heads were segmented under the base of CT images (Fig. 3a), high radioactivity from other bones (i.e., acetabulum) often encroached on the photopenic femoral heads (Fig. 3b). Thus, in most cases, it was difficult to demarcate the true femoral head activity free from the surrounding bone on the SPECT/CT images (Fig. 3c).

SPECT/CT Parameters of the Femoral Neck

The femoral neck fracture sites always revealed variable degree of increased uptake, but the quantitative parameters over the fracture site are not presented because increased uptake of the fracture site is already expected and we wanted to investigate potential abnormalities of the intact contralateral femoral neck. The statistical analyses showed that the femoral necks from the contralateral side had significantly greater SUVmean (3.17 ± 1.20 vs. 2.32 ± 0.53 , $p = 0.021$) and SUVmin (1.64 ± 0.63 vs. 1.04 ± 0.27 ; $p = 0.002$) than those from controls (Fig. 4; Table 2). Same tendency was observed for the SUVmax without a statistical significance (4.91 ± 1.98 vs. 3.97 ± 1.07 ; $p = 0.138$).

Cutoff Value of SUVmin for Detection of Non-viable Femoral Head

The SUVmin was the most consistent parameter for detection of a non-viable femoral head (Figs. 2 and 3); thus, we performed ROC curve analysis for detection/exclusion of osteonecrosis using the SUVmin compared with the controls. The area-under-the-curve (AUC) was 0.815 with a 95% confidence interval of 0.661–0.920 ($p = 0.006$). As a result, the optimal cutoff SUVmin for detection of osteonecrosis was 0.61 (g/mL) with a sensitivity of 77.8% and a specificity of 87.1% (Fig. 5).

Discussion

In the current study, a novel quantitative parameter of SPECT/CT, minimum SUV (SUVmin), was proved to be useful for the diagnosis of femoral head osteonecrosis in patients with femoral neck fracture. The SUVmin denotes the lowest SUV in terms of a voxel in a given region, and it was significantly reduced in the osteonecrotic femoral heads compared to that in normal controls and contralateral femoral heads (Fig. 2c). The SUVmax (the highest SUV in terms of a voxel) and SUVmean (the average SUV over the given

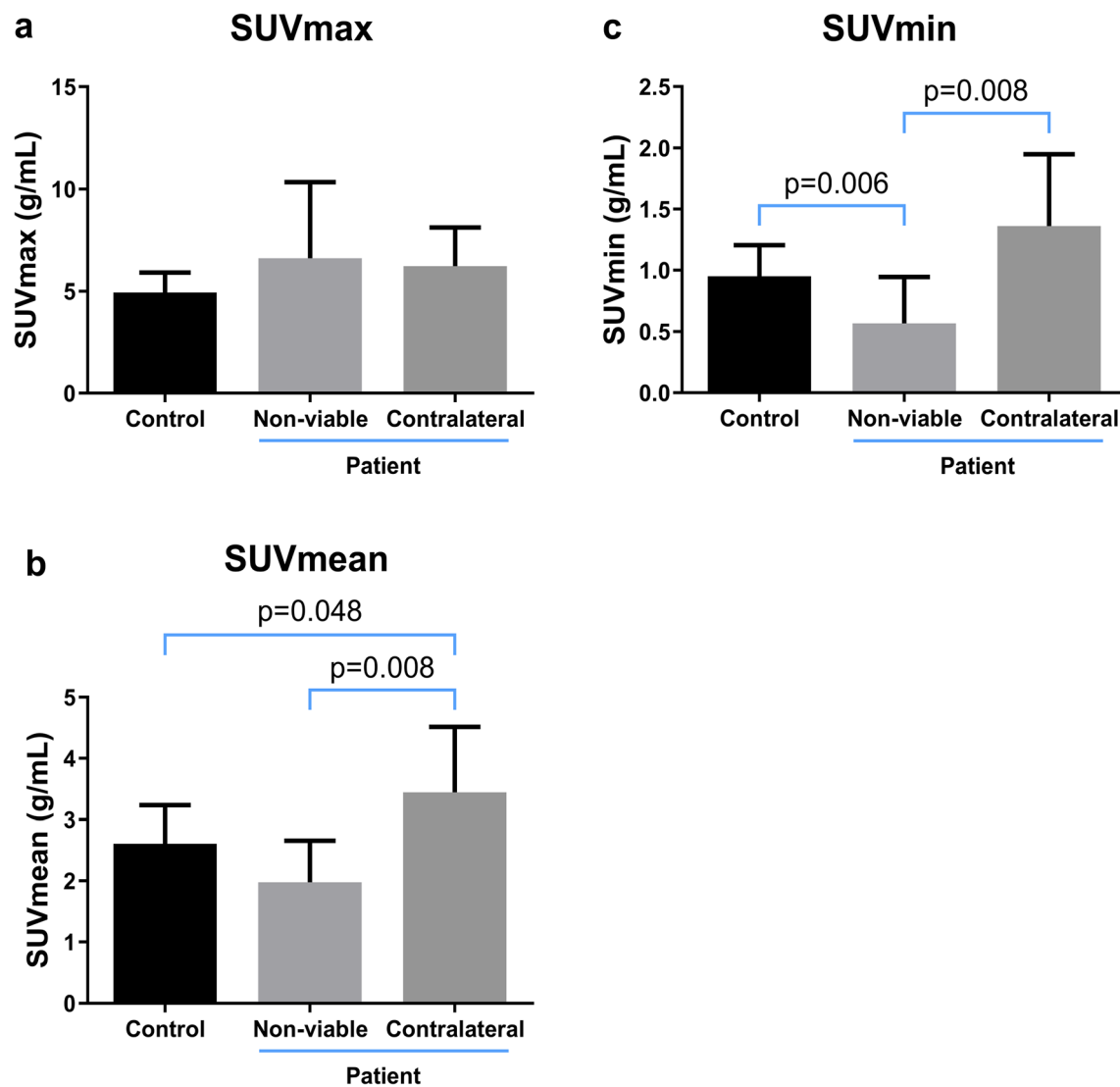


Fig. 2 SPECT/CT parameters of the femoral head. **a** SUVmax, **b** SUVmean, and **c** SUVmin. Control: SUV average of the bilateral femoral heads of controls. Non-viable: SUV of the femoral head with osteonecrosis. Contralateral: SUV of the contralateral femoral head without osteonecrosis

region) were not consistently reduced in the non-viable femoral heads (Fig. 2a, b). These findings suggest that a voxel with the lowest SUV may properly assess tissue

viability. In other words, the “normal activity” of healthy tissue may be readily reflected by the voxel of the lowest SUV.

Table 1 SPECT/CT parameters of the femoral heads

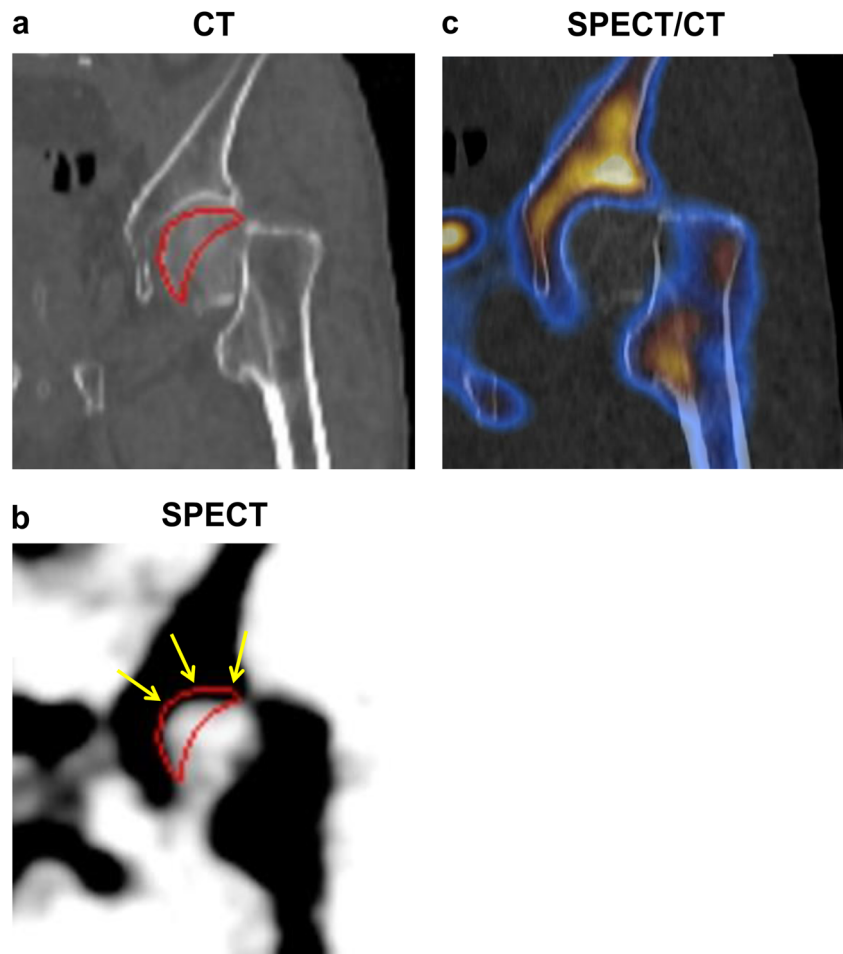
SPECT/CT parameters	Controls ($n = 31$) (mean \pm SD)	Patients with femoral neck fracture ($n = 9$) (mean \pm SD)	
		Non-viable	Contralateral
SUVmax (g/mL)	4.94 \pm 0.97	6.60 \pm 3.74	6.21 \pm 1.90
SUVmean (g/mL)	2.61 \pm 0.63	1.98 \pm 0.68	3.44 \pm 1.07
SUVmin (g/mL)	0.95 \pm 0.26	0.57 \pm 0.38	1.36 \pm 0.59

Control: SUV average of the bilateral femoral heads of controls

Non-viable: SUV of the femoral head with osteonecrosis

Contralateral: SUV of the contralateral femoral head without osteonecrosis

Fig. 3 Spill-over effect on the femoral head demonstrated by SPECT/CT of a 91-year-old male patient with osteonecrosis of the left femoral head. The red contour denotes the femoral head segmentation on CT image (a). The radioactivity from the acetabulum (yellow arrows) invaded the photopenic femoral head (b). The ball-and-socket structure of the hip joint made it difficult to identify the true femoral head activity on the SPECT/CT fusion image (c)



Those findings contrast with the high utility of SUVmax from quantitative bone SPECT/CT for evaluating “abnormal activity” of disease [10, 12, 18]; the disease activity was effectively represented by a voxel of the highest SUV. If SUVmin had been tested for the evaluation of bone/joint diseases, the inclusion of the non-disease component within a given VOI would have resulted in an erroneous SUVmin, and ultimately underestimated the disease activity. In fact, this effect impaired the diagnostic efficacy of SUVmean for TMD detection, because the true disease activity and non-disease activity were averaged [10].

Regarding “normal activity” of healthy tissue, such as femoral head viability, it could not be properly assessed by the SUVmax, because the extra-component within the VOI (i.e., activity from the adjacent acetabula bone or femoral neck fracture itself) resulted in overestimation of the “normal activity” of the femoral head (Fig. 3). This phenomenon also influenced the SUVmean because the activities from the femoral head and other bones were averaged. The surrounding activity might also interfere with the true SUVmin (the lowest SUV in a given VOI) within the femoral head, but the second, third, or next lowest SUVmin would still remain to represent the

“normal activity” of the femoral head. Traditionally, the scintigraphic diagnosis of osteonecrosis has been dependent on the identification of the photon-deficit area [3–6]. The uptake of bone agents over the entire femoral head (typical volume of 20–30 mL) has been determined by visual assessment. In the current study, the voxel volume for SUVmin was just $3.2\text{--}7.3 \times 10^{-3}$ mL. The radioactivity in such a small VOI may be affected by other image acquisition/reconstruction conditions. Therefore, keeping the constant protocol is of paramount importance to maintain reliability. A large scale multi-center study is crucial in this regard.

The innocent contralateral femoral necks of femoral neck fracture patients showed greater SUVs compared to the controls (Fig. 4) but the underlying cause was not fully addressed in the current study. The strenuous weight-bearing of the contralateral lower extremity may be one of the causes of the high uptake of bone agents [19, 20]. Age-dependent osteoporosis, which has been reported to increase the uptake of bone scintigraphy agents over the femoral neck and shaft [21], may explain the high SUVs of the contralateral femoral necks: the patients with femoral neck fracture were significantly older than the controls (mean 79.3 years vs. 45.7 years) in

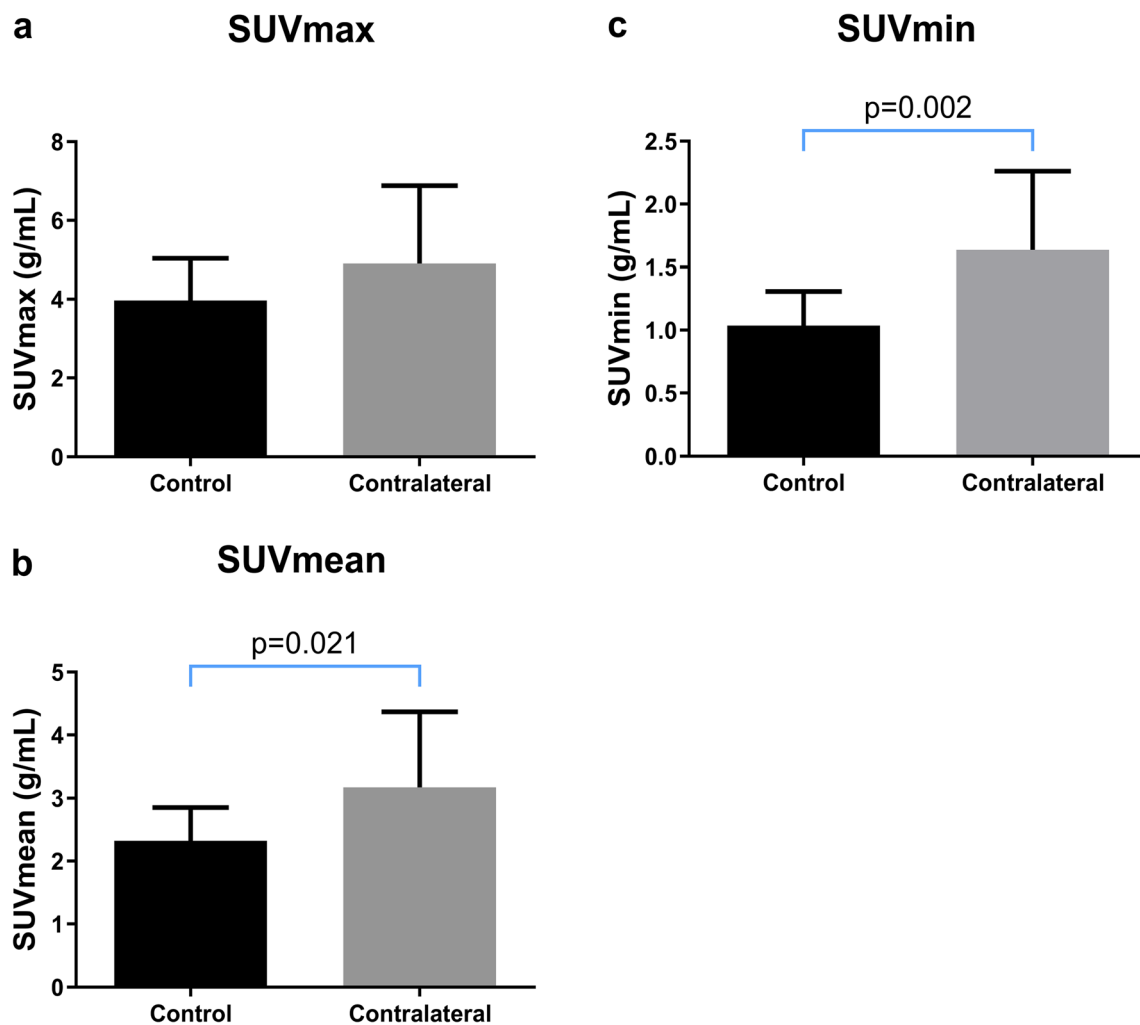


Fig. 4 SPECT/CT parameters of the femoral neck. **a** SUVmax, **b** SUVmean, and **c** SUVmin. Control: SUV average of the bilateral femoral necks of controls. Contralateral: SUV of the contralateral femoral neck of patients

the current study. As a matter of fact, the high bone uptake of Tc-99m labeled diphosphonates has been considered to be a useful non-invasive indicator for the assessment of bone loss (bone turn-over) in osteoporosis [22] and metabolic bone diseases [23]. Further studies are required to investigate the SUV changes in deranged conditions of bone metabolism.

There are some limitations of this study. The retrospective design with limited number of enrolled cases is a critical weak point of the study. Comparison with other imaging modalities like MRI [24, 25] was beyond the scope of the current study. Prognostic implications of the SUVmin in femoral head osteonecrosis should be evaluated in further studies.

Table 2 SPECT/CT parameters of femoral necks excluding the fracture site

SPECT/CT parameters	Controls ($n = 31$) (mean \pm SD)	Patients with femoral neck fracture (contralateral femoral neck, $n = 9$) (mean \pm SD)
SUVmax (g/mL)	3.97 \pm 1.07	4.91 \pm 1.98
SUVmean (g/mL)	2.32 \pm 0.53	3.17 \pm 1.20
SUVmin (g/mL)	1.04 \pm 0.27	1.64 \pm 0.63

Control: SUV average of the bilateral femoral necks of controls

Contralateral: SUV of the contralateral femoral neck of patients

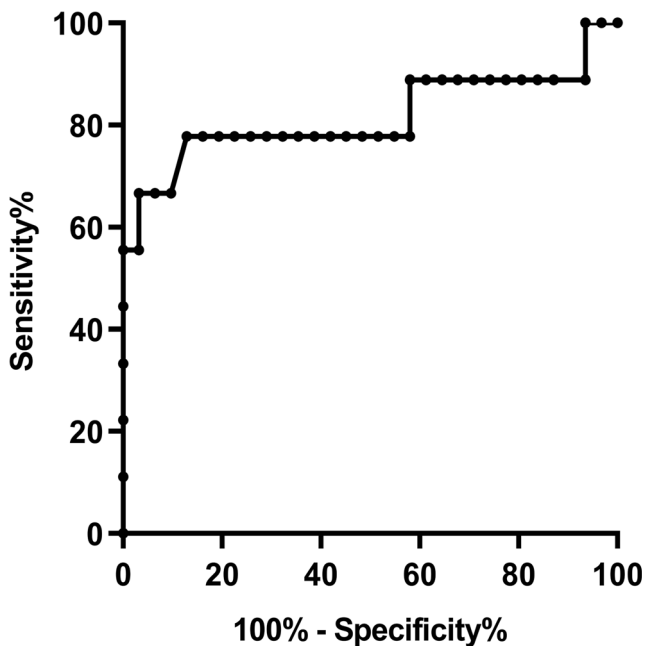


Fig. 5 ROC curve analysis using SUVmin for detection/exclusion of non-viable femoral head. The cutoff SUVmin of 0.61 (g/mL) yielded the sensitivity of 77.8% and specificity of 87.1% (area-under-the-curve = 0.815; 95% confidence interval = 0.661–0.920; $p = 0.006$)

Conclusion

Quantitative bone SPECT/CT is promising for the evaluation of femoral head viability in patients with femoral neck fracture. The novel quantitative parameter, minimum SUV, may play a role in the objective and unbiased assessment of femoral head viability with a cutoff value of 0.61 (g/mL).

Compliance with Ethical Standards

Conflict of Interest Hyun Gee Ryoo, Won Woo Lee, Ji Young Kim, Eunjung Kong, Woo Hee Choi, and Joon-Keo Yoon declare that there is no conflict of interest. This study was supported in part by the Basic Science Research Program through the National Research Foundation of Korea funded by the Ministry of Education (2018R1D1A1A09081961) and by the Korean Society of Nuclear Medicine Clinical Trial Network (KSNM CTN) working group funded by the Korean Society of Nuclear Medicine (KSNM-CTN-2017-01-01).

Ethical Approval The study was approved by an institutional review board and has been performed in accordance with the ethical standards laid down in the 1964 Declaration of Helsinki and its later amendments.

Informed Consent The need for informed consents was waived by the institutional review board.

References

1. Lewis SL, Rees JJ, Thomas GV, Williams LA. Pitfalls of bone scintigraphy in suspected hip fractures. *Br J Radiol.* 1991;64:403–8.

2. Sarikaya I, Sarikaya A, Holder LE. The role of single photon emission computed tomography in bone imaging. *Semin Nucl Med.* 2001;31:3–16.
3. Collier BD, Carrera GF, Johnson RP, Isitman AT, Hellman RS, Knobel J, et al. Detection of femoral head avascular necrosis in adults by SPECT. *J Nucl Med.* 1985;26:979–87.
4. Ryu JS, Kim JS, Moon DH, Kim SM, Shin MJ, Chang JS, et al. Bone SPECT is more sensitive than MRI in the detection of early osteonecrosis of the femoral head after renal transplantation. *J Nucl Med.* 2002;43:1006–11.
5. Luk WH, Au-Yeung AW, Yang MK. Diagnostic value of SPECT versus SPECT/CT in femoral avascular necrosis: preliminary results. *Nucl Med Commun.* 2010;31:958–61.
6. Agarwal KK, Mukherjee A, Sharma P, Bal C, Kumar R. Incremental value of ^{99m}Tc -MDP hybrid SPECT/CT over planar scintigraphy and SPECT in avascular necrosis of the femoral head. *Nucl Med Commun.* 2015;36:1055–62.
7. Han S, Oh M, Yoon S, Kim J, Kim JW, Chang JS, et al. Risk stratification for avascular necrosis of the femoral head after internal fixation of femoral neck fractures by post-operative bone SPECT/CT. *Nucl Med Mol Imaging.* 2017;51:49–57.
8. Bailey DL, Willowson KP. An evidence-based review of quantitative SPECT imaging and potential clinical applications. *J Nucl Med.* 2013;54:83–9.
9. Bailey DL, Willowson KP. Quantitative SPECT/CT: SPECT joins PET as a quantitative imaging modality. *Eur J Nucl Med Mol Imaging.* 2014;41(Suppl 1):S17–25.
10. Suh MS, Lee WW, Kim YK, Yun PY, Kim SE. Maximum standardized uptake value of (^{99m}Tc) Hydroxymethylene diphosphonate SPECT/CT for the evaluation of temporomandibular joint disorder. *Radiology.* 2016;280:890–6.
11. Lee H, Kim JH, Kang YK, Moon JH, So Y, Lee WW. Quantitative single-photon emission computed tomography/computed tomography for technetium pertechnetate thyroid uptake measurement. *Medicine (Baltimore).* 2016;95:e4170.
12. Kim J, Lee HH, Kang Y, Kim TK, Lee SW, So Y, et al. Maximum standardised uptake value of quantitative bone SPECT/CT in patients with medial compartment osteoarthritis of the knee. *Clin Radiol.* 2017;72:580–9.
13. Kim HJ, Bang JI, Kim JY, Moon JH, So Y, Lee WW. Novel application of quantitative single-photon emission computed tomography/computed tomography to predict early response to Methimazole in Graves' disease. *Korean J Radiol.* 2017;18:543–50.
14. Kang YK, Park S, Suh MS, Byun SS, Chae DW, Lee WW. Quantitative single-photon emission computed tomography/computed tomography for glomerular filtration rate measurement. *Nucl Med Mol Imaging.* 2017;51:338–46.
15. Kim JY, Kim JH, Moon JH, Kim KM, Oh TJ, Lee DH, et al. Utility of quantitative parameters from single-photon emission computed tomography/computed tomography in patients with destructive thyroiditis. *Korean J Radiol.* 2018;19:470–80.
16. Kim J, Lee H, Lee H, Bang JI, Kang YK, Bae S, et al. Quantitative single-photon emission computed tomography/computed tomography for evaluation of salivary gland dysfunction in Sjogren's syndrome patients. *Nucl Med Mol Imaging.* 2018;52:368–76.
17. Lee R, So Y, Song YS, Lee WW. Evaluation of hot nodules of thyroid gland using ^{99m}Tc Pertechnetate: a novel approach using quantitative single-photon emission computed tomography/computed tomography. *Nucl Med Mol Imaging.* 2018;52:468–72.
18. Bae S, Kang Y, Song YS, Lee WW, Group KS. Maximum standardized uptake value of foot SPECT/CT using ^{99m}Tc HDP in patients with accessory navicular bone as a predictor of surgical treatment. *Medicine (Baltimore).* 2019;98:e14022.
19. Casara D, de Besi P, Fiorentino M, Fornasiero A, Melanotte P, Palu G, et al. False positive bone scan in bone tumors of the lower limb. *Eur J Nucl Med.* 1977;2:179–81.

20. Lee WW, Kim TU, Kim TH, Jung CY, Moon JH. Usefulness of three-phasic bone scan in young male patients suspected of post-traumatic reflex sympathetic dystrophy syndrome. *Nucl Med Mol Imaging*. 2001;35:52–60.
21. Israel O, Lubushitzky R, Frenkel A, Iosilevsky G, Bettman L, Gips S, et al. Bone turnover in cortical and trabecular bone in normal women and in women with osteoporosis. *J Nucl Med*. 1994;35:1155–8.
22. Fogelman I, Bessent RG, Cohen HN, Hart DM, Lindsay R. Skeletal uptake of diphosphonate. Method for prediction of postmenopausal osteoporosis. *Lancet*. 1980;2:667–70.
23. Israel O, Front D, Hardoff R, Ish-Shalom S, Jerushalmi J, Kolodny GM. In vivo SPECT quantitation of bone metabolism in hyperparathyroidism and thyrotoxicosis. *J Nucl Med*. 1991;32:1157–61.
24. Markisz JA, Knowles RJ, Altchek DW, Schneider R, Whalen JP, Cahill PT. Segmental patterns of avascular necrosis of the femoral heads: early detection with MR imaging. *Radiology*. 1987;162:717–20.
25. Beltran J, Herman LJ, Burk JM, Zuelzer WA, Clark RN, Lucas JG, et al. Femoral head avascular necrosis: MR imaging with clinical-pathologic and radionuclide correlation. *Radiology*. 1988;166:215–20.

Publisher's Note Springer Nature remains neutral with regard to jurisdictional claims in published maps and institutional affiliations.